INCLUSIVE MEASUREMENTS OF DIFFRACTION IN DEEP-INELASTIC SCATTERING AND PHOTOPRODUCTION [a]

P.R. NEWMAN
School of Physics and Space Research, University of Birmingham, B15 2TT, England.

A precision measurement of diffractive deep-inelastic ep scattering is presented in the form of the structure function, $F_2^{D(3)}(\beta, Q^2, x_{I\!P})$. Factorisation of the $x_{I\!P}$ dependence is found to be broken. The Q^2 and β dependences are examined after averaging $F_2^{D(3)}$ over $x_{I\!P}$. Unambiguous violations of scale invariance are observed. Perturbative QCD fits based on DGLAP evolution favour a "leading" gluon distribution carrying in excess of 80% of the momentum of the exchange. Also presented is the differential cross-section, $d\sigma^D/dM_X^2$ for diffractive photoproduction processes in which the proton remains intact and a system of mass M_X is produced at the photon vertex. It displays a quasi-elastic peak and a higher mass continuum, both of which are consistent with Regge predictions based on a soft pomeron.

1 Introduction

Following the observation at HERA in 1992 of deep-inelastic scattering (DIS) events with a large region of rapidity around the proton remnant direction devoid of hadron production,[1,2] data taken in 1993 were used to quantify the contribution of such events to the DIS cross-section, by the measurement of a structure function $F_2^{D(3)}$.[3,4] This demonstrated that the rapidity gap events could dominantly be attributed to diffraction and gave the first indications of a large gluonic contribution to the partonic sub–structure of the exchange.[5,6] Considerably more precise 1994 preliminary H1 results on the diffractive structure function in an extended kinematic range are presented here.

Results from HERA on the total γp cross-section,[7,8] and exclusive light vector meson photoproduction [9,10] have been well described in the Regge picture in terms of a single pomeron trajectory, consistent with that obtained by Donnachie and Landshoff in fits to pp and $\bar{p}p$ total cross-sections.[11] The first inclusive measurements of the invariant mass distribution of the products of diffraction dissociation of real photons at HERA energies are also presented here.

[a] First presented at the Topical Conference on Hard Diffraction, Eilat, Israel, February 1996.

2 Diffractive Deep-Inelastic Scattering

2.1 Experimental Method

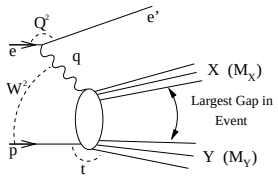

Figure 1: Schematic illustration of the method of decomposing events to define diffractive cross-sections, showing the kinematic variables discussed in the text.

The measured cross-section is defined in terms of the generalised process, $ep \to e'XY$, illustrated in figure 1. The hadronic final state in any event may be decomposed into two systems, X and Y, that are separated by the largest gap in the rapidity distribution of hadrons in the $\gamma^\star p$ centre of momentum frame. A cross-section is then measured at different values of the masses, $M_{_X}$ and $M_{_Y}$, of the two systems. When both masses are small by comparison with the centre of mass energy, a large rapidity gap must always occur from kinematic considerations alone, and the t-channel diffractive exchange dominates the process, $\gamma^\star p \to XY$.

With q and P denoting 4-vectors for the virtual photon and the proton respectively and with X and Y denoting 4-vectors for the two distinct components of the hadronic final state, we define the standard kinematic variables

$$Q^2 = -q^2 \quad W^2 = (q+P)^2 \quad t = (P-Y)^2 \quad x_{I\!P} = \frac{Q^2+X^2}{Q^2+W^2} \quad \beta = \frac{Q^2}{Q^2+X^2}$$

The experimental selection of events is based on the presence of a rapidity gap spanning at least the laboratory range $3.0 < \eta < 7.5$, inferred from the absence of activity in the forward[b] components of the H1 detector.[12] The event kinematics are obtained by reconstructing $M_{_X}$ using all particles produced backward of the gap and from the measurement of a scattered electron in the Backward Electromagnetic Calorimeter.[12] The lower limit of 7.5 on the rapidity reached by particles in the leading baryonic system Y restricts its mass to $M_{_Y} \lesssim 1.6$ GeV and implies that $|t| \lesssim 1.0$ GeV^2. This system is not directly observed, though by requiring $x_{I\!P} < 0.05$, we ensure that Y carries in excess of 95% of the incident proton momentum. Any isospin-exchanging process is strongly suppressed in this kinematic region. The contribution to the

[b] The forward direction is defined to be that of the outgoing proton beam, and corresponds to positive rapidities.

measured cross-section from events in which the proton dissociates is estimated to be at the level of 5% using the DIFFVM [14] Monte Carlo.

The data presented here correspond to an integrated luminosity of 2.0 pb^{-1}: a ten-fold increase in statistics compared to our earlier measurement.[3] A further 0.06 pb^{-1} of data taken with the interaction point shifted by 70 cm in the forward (proton) direction enable measurements to be made at lower values of Q^2 than has previously be possible.

2.2 The Diffractive Structure Function, $F_2^{D(3)}(\beta, Q^2, x_{I\!P})$

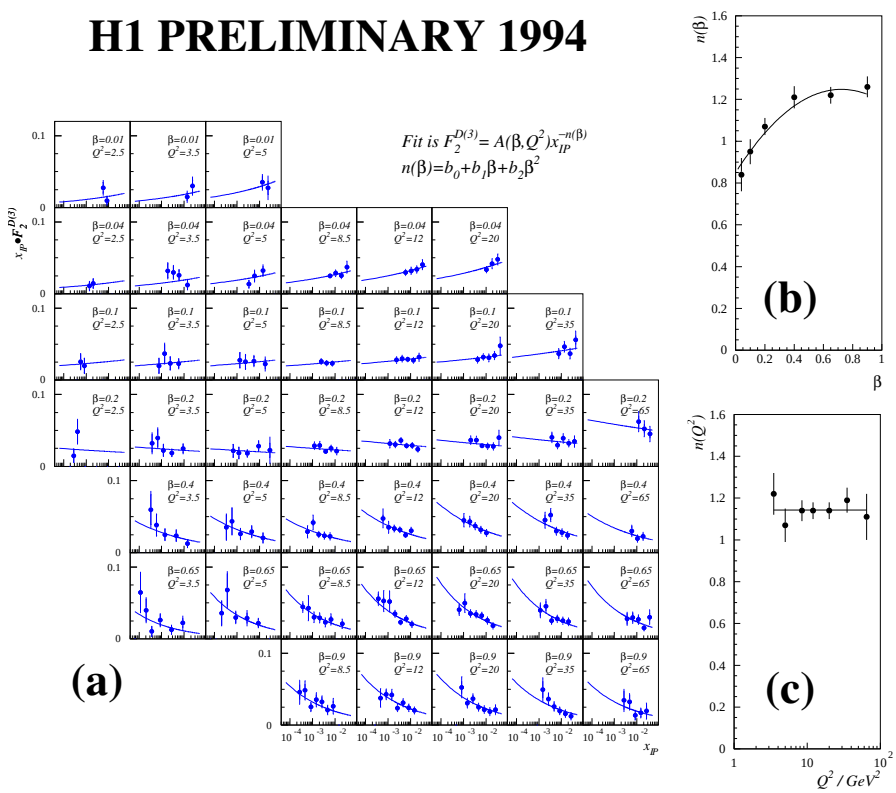

Figure 2: (a) $x_{I\!P} \cdot F_2^{D(3)}(\beta, Q^2, x_{I\!P})$ integrated over the range $M_Y < 1.6$ GeV and $|t| < 1$ GeV^2. (b) The β dependence of n when $F_2^{D(3)}$ is fitted to the form $F_2^{D(3)} = A(\beta, Q^2)/{x_{I\!P}}^{n(\beta)}$. (c) The Q^2 dependence of n when $F_2^{D(3)}$ is fitted to the form $F_2^{D(3)} = A(\beta, Q^2)/{x_{I\!P}}^{n(Q^2)}$. The experimental errors are statistical and systematic added in quadrature. The overall fit described in the text is shown in all three plots.

Following the proposal of Ingelman and Schlein,[13] the results are presented

in terms of a diffractive structure function, $F_2^{D(3)}(\beta, Q^2, x_{I\!P})$, which is related to the differential $ep \to e'XY$ cross section by

$$\frac{\mathrm{d}^3\sigma^D_{ep\to eXY}}{\mathrm{d}x_{I\!P}\,\mathrm{d}\beta\,\mathrm{d}Q^2} = \frac{4\pi\alpha^2}{\beta Q^4}(1 - y + \frac{y^2}{2})F_2^{D(3)}(\beta, Q^2, x_{I\!P}). \quad (1)$$

The quantity, $x_{I\!P} \cdot F_2^{D(3)}(\beta, Q^2, x_{I\!P})$ is shown as a function of $x_{I\!P}$ in figure 2a, in the kinematic range $2.5 < Q^2 < 65$ GeV^2, $0.01 < \beta < 0.9$ and $0.0001 < x_{I\!P} < 0.05$. In a Regge interpretation [15] in which the $x_{I\!P}$ dependence describes a pomeron flux associated with the proton, one expects a behaviour of the form, $F_2^{D(3)} \propto \frac{1}{x_{I\!P}^n}$, with $n \simeq 2\alpha(0) - 1$, where $\alpha(t) = \alpha(0) + \alpha' t$ is the pomeron trajectory [c]. Figure 2b shows the results of a fit to this form when n is allowed to vary with β but not with Q^2. The improved precision and enhanced kinematic range reveal deviations from the universal factorisation previously reported,[3] with n decreasing significantly with β for $\beta \lesssim 0.3$. The value of n at $\beta \gtrsim 0.3$ is slightly larger than that expected for a soft pomeron.[11] There are a number of potential explanations for the decrease in n for $\beta \lesssim 0.2$ to values below unity. One possibility is that there is a contribution from the exchange of meson trajectories (f, a_2 etc.), which have lower intercepts and softer β dependences than the leading vacuum trajectory. In a partonic interpretation of the diffractive exchange (see section 2.3), such an effect may occur if the β or $x_{I\!P}$ dependence differs for sea quark and gluon components of the exchange.[16]

In figure 2c, n is allowed to vary with Q^2 but not β. There is no evidence for any dependence of n on $\ln Q^2$. A purely illustrative, though acceptable fit in which the value of n varies quadratically with β and has no Q^2 dependence is superimposed in figures 2a–c.

2.3 The Partonic Structure of Diffractive Exchange

Integrating $F_2^{D(3)}$ over a fixed range in $x_{I\!P}$ yields a quantity which is proportional to the average structure function of whatever colourless exchanges contribute to the measured cross-section in the kinematic range accessed. We define

$$\tilde{F}_2^D(\beta, Q^2) = \int_{x_{I\!P}=0.0003}^{x_{I\!P}=0.05} F_2^{D(3)}(\beta, Q^2, x_{I\!P})\mathrm{d}x_{I\!P} \quad (2)$$

[c] In practice, the finite values of t at which the measurement takes place reduce n relative to $2\alpha(0) - 1$ by a few percent.

Where no measurement has been made, the fit shown in figure 2 is used to make extrapolations.

Fig. 3a shows $\tilde{F}_2^D(\beta, Q^2)$ as a function of Q^2 for fixed β and fig. 3b shows it as a function of β for fixed Q^2. No fast variation with Q^2 is observed, though violations of scaling are clearly established. A rise with $\ln Q^2$ persists to values of β far in excess of the point ($x \sim 0.15$) at which the structure of the nucleon is dominated by valence quarks rather than by gluons and $\frac{\partial F_2(x,Q^2)}{\partial \ln Q^2}$ correspondingly becomes negative.[17] The scaling violations of $\tilde{F}_2^D(\beta, Q^2)$ are thus in qualitative accord with the hypothesis of a substantial hard gluon component in the structure of the diffractive exchange. At fixed Q^2, $\tilde{F}_2^D(\beta, Q^2)$ displays little dependence on β. There is no evidence for the fall with increasing parton momentum fraction characteristic of hadron structure functions. A

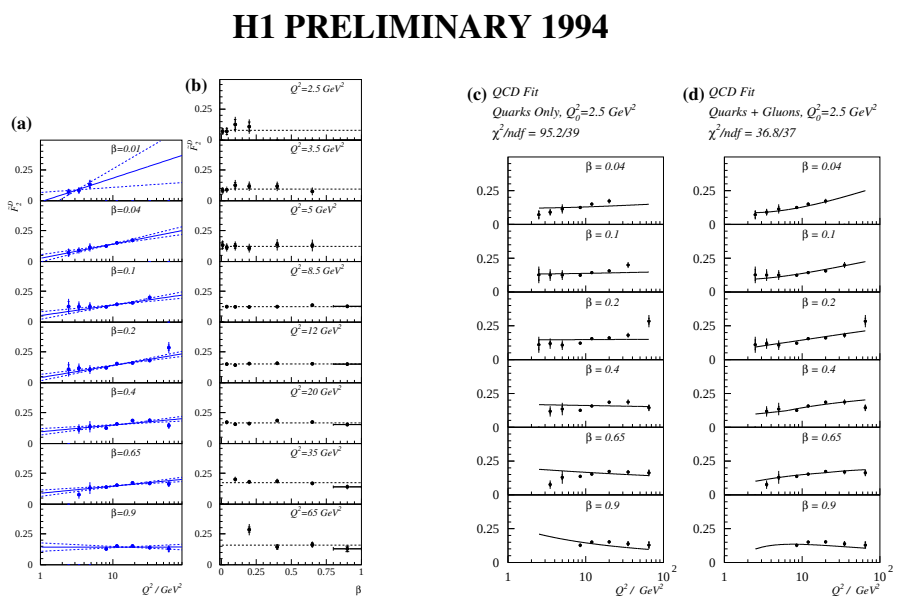

Figure 3: (a) $\tilde{F}_2^D(\beta, Q^2)$ as a function of Q^2 for different β values. The superimposed lines correspond to the best fit to a linear dependence on $\ln Q^2$ (continuous) and $\pm 1\sigma$ (dashed). (b) $\tilde{F}_2^D(\beta, Q^2)$ as a function of β for different Q^2 values, with a best fit to a constant β dependence. c) DGLAP QCD comparison of the (β, Q^2) dependence of $\tilde{F}_2^D$ assuming only quarks at the starting scale of $Q_0^2 = 2.5\,\mathrm{GeV}^2$; d) DGLAP QCD comparison of the (β, Q^2) dependence of $\tilde{F}_2^D$ assuming both quarks and gluons at the starting scale.

QCD analysis of $\tilde{F}_2^D(\beta, Q^2)$ confirms this qualitative picture.[5,6,18] A u+d+s flavour singlet quark and a gluon distribution are parameterised at a starting

scale, $Q_0^2 = 2.5\ \mathrm{GeV}^2$, as

$$x_{i/I\!P} \cdot f_i(x_{i/I\!P}) = A_i\ x_{i/I\!P}^{B_i}\ (1 - x_{i/I\!P})^{C_i} \tag{3}$$

where $i = q, g$ and $x_{i/I\!P}$ is the fraction of the exchange momentum carried by the parton. These parton distributions are evolved using DGLAP [19] evolution to $Q^2 > Q_0^2$, with the values of $A_{q,g}$, $B_{q,g}$ and $C_{q,g}$ as fit parameters [d]. Charm quarks are not explicitly introduced into the parton distributions, but are included through boson-gluon fusion using the procedure followed in [21].

Figure 3c shows the best fit obtained for $\tilde{F}_2^D$ when A_g is constrained to be zero, and only quarks contribute at the starting scale. Because of the persistence of rising $\ln Q^2$ scaling violations to high values of β, no such parameterisation is acceptable. An excellent fit, shown in figure 3d, can be obtained when gluons are also introduced at the starting scale.

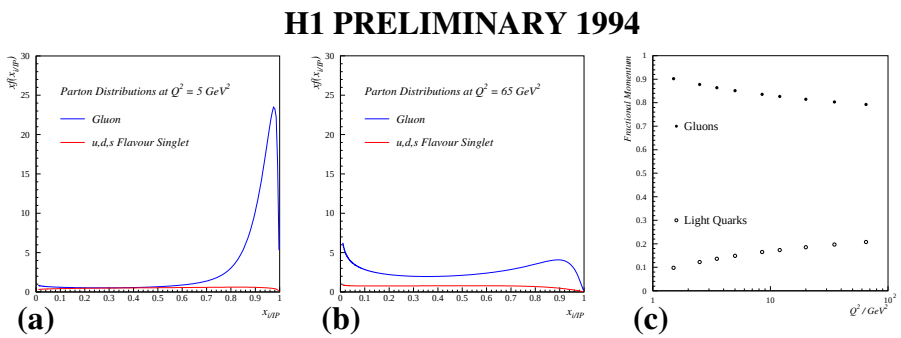

Figure 4: Quark and gluon momentum weighted distributions in fractional momenta $x_{g/I\!P}$ and $x_{q/I\!P}$ for diffractive exchange averaged over $x_{I\!P}$ and t extracted using the DGLAP QCD fit at (a) $Q^2 = 5\ \mathrm{GeV}^2$ and (b) $Q^2 = 65\ \mathrm{GeV}^2$; c) fraction of the total momentum transfer carried by quarks and by gluons at each Q^2; no errors are shown in the plots because of ambiguity in their determination due to the tendency of the solution to peak at large $x_{g/I\!P}$.

The parton densities in the mixed quark and gluon fit at $Q^2 = 5\ \mathrm{GeV}^2$ and $Q^2 = 65\ \mathrm{GeV}^2$ are shown in figure 4, along with the integrated momentum fractions carried by quarks and gluons as a function of Q^2. At $Q^2 = 5\ \mathrm{GeV}^2$, a "leading" gluon behaviour is observed, in which the exchange is dominated by gluons carrying fractional momentum, $x_{g/I\!P} > 0.9$, tending to a singularity as $x_{g/I\!P} \to 1$. As Q^2 increases, the gluon distribution in the solution evolves in the usual way to lower values of β. Throughout the Q^2 range, in excess

[d] Since additional theoretical input is required to normalise the structure function, and since it is far from clear that one should exist for space-like exchanges [20], no momentum sum rule is imposed.

of 80% of the exchange momentum is carried by gluons. H1 analyses of the hadronic final state in diffractive DIS lend support to these conclusions[22]. The "leading" gluon behaviour is expected in models of deep–inelastic diffraction such as that proposed by Buchmüller and Hebecker.[23]

3 Diffraction in Photoproduction

Similar techniques [24] to those employed in the DIS case have been used to measure inclusive cross-sections for diffractive photoproduction at a γp centre of mass energy averaged over the photon flux of $\langle W \rangle = 187$ GeV. Figure 5

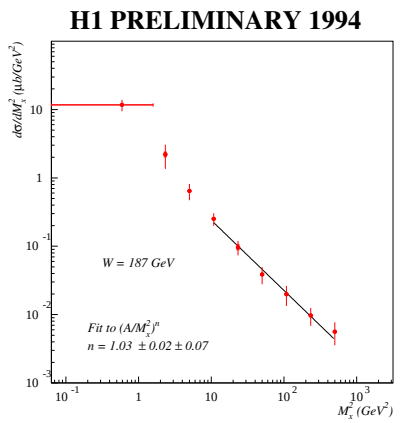

Figure 5: Corrected points obtained for the t-integrated cross-section, $d\sigma^D/dM_X^2\,(\gamma p \to Xp)$ at $Q^2 = 0$ and $\langle W \rangle = 187$ GeV. A fit to the form, $(1/M_X^2)^n$ is shown for $10.8 < M_X^2 < 500$ GeV^2.

shows the t–integrated cross-section, $d\sigma^D/dM_X^2$ for photoproduction processes that are elastic at the proton vertex[e]. In the "triple Regge" region ($M_X^2 \to \infty$, $W^2/M_X^2 \to \infty$), the dynamics of dissociation processes have been shown [25] to be well described by combinations of triple Regge amplitudes, which at low values of M_X^2/W^2 are dominated by the triple pomeron amplitude.[26] Assuming that the triple pomeron diagram dominates and parameterising the product of the triple pomeron coupling and the couplings of the pomeron to external particles[f] by $e^{b_0 t}$, the differential cross-section is expected to behave at fixed W as [15]

[e] A correction at the level of 5% is made to remove proton dissociative events.

[f] In the measured region, the minimum kinematically permissible value of $|t|$ is close to zero.

$$\frac{d\sigma^D}{dM_X^2} \sim \left(\frac{1}{M_X^2}\right)^{\alpha(0)} \cdot \left(b_0 + 2\alpha' \ln \frac{W^2}{M_X^2}\right)^{-1} \qquad (4)$$

For $10.8 < M_X^2 < 500$ GeV^2, a fit to the form, $\frac{d\sigma^D}{dM_X^2} \sim (1/M_X^2)^n$ is shown in figure 5. The result of the fit is $n = 1.03 \pm 0.02$(stat.) ± 0.07(syst.), illustrating that the data display the approximate $1/M_X^2$ dependence characteristic of diffractive dissociation. A fit to the full form of equation 4 yields $\alpha(0) = 1.11 \pm 0.02$(stat.) ± 0.07(syst.), where we have taken $\alpha' = 0.25$ GeV^{-2} and $b_0 = 3 \pm 1$ GeV^{-2}, estimated from fixed target data.[27] This result confirms that the dominant contribution to the cross-section for the dissociation of photons to low mass states arises from the triple pomeron amplitude. The proximity of the extracted $\alpha(0)$ to the established value of 1.08 [11] also provides a control for the measurement of F_2^D.

Monte Carlo models are used to unfold the points in figure 5 to separate total cross-sections for quasi-elastic and dissociative diffractive photoproduction processes. We obtain $\sigma(\gamma p \to Vp) = 18.2 \pm 0.8$(stat.) ± 2.8(syst.) μb, where $V = \rho^0$, ω or ϕ, and $\sigma(\gamma p \to Xp) = 21.5 \pm 0.6$(stat.) ± 5.9(syst.) μb where X is any other state with $M_X^2/W^2 < 0.05$. These measurements confirm our previous results [7] and uncertainties are reduced.

4 Summary and Conclusions

Diffractive deep-inelastic ep scattering at HERA has been investigated using the data taken in 1994 with the H1 detector. At the present level of experimental precision, the dependence on $x_{I\!P}$ of the diffractive structure function, $F_2^{D(3)}(\beta, Q^2, x_{I\!P})$, is found to vary with β but not with Q^2. The scaling violations in the Q^2 dependence of $\tilde{F}_2^D(\beta, Q^2)$ for fixed β are shown to be interpretable in the framework of QCD in terms of parton densities that are dominated by a gluon distribution that peaks strongly as $x_{g/I\!P} \to 1$ and carries approximately 80% of the momentum of the diffractive exchange.

A measurement of the invariant mass distribution of the component of the final state produced at the photon vertex in diffractive photoproduction processes where the proton remains intact shows a peak in the region of the light vector mesons, ρ, ω and ϕ and a dissociation continuum at larger masses. In the triple Regge region, the cross-section is in good agreement with a prediction based on the triple pomeron amplitude.

Acknowledgements

We are grateful to the HERA machine group and to H1's engineers and technicians for their work in constructing and now maintaining the HERA accelerator and the H1 detector. We thank our funding agencies for financial support, the DESY technical staff for continual assistance, and the DESY directorate for the hospitality which they extend to the non–DESY members of the collaboration. The author wishes to acknowledge the help of many members of the H1 collaboration with the preparation of this contribution.

References

1. ZEUS Collaboration, M. Derrick et al., Phys. Lett. **B315** (1993) 481.
2. H1 Collaboration, T. Ahmed et al., Nucl. Phys. **B429** (1994) 477.
3. H1 Collaboration, T. Ahmed et al., Phys. Lett. **B348** (1995) 681.
4. ZEUS Collaboration, M. Derrick et al., Z. Phys **C68** (1995) 569.
5. J. Phillips, "Rapidity Gap Events at HERA and the Structure of the Pomeron", in Proc. of the International Workshop on Deep–Inelastic Scattering and Related Topics, Paris, France, April 1995, p.359.
6. J. Dainton, "Deep–Inelastic Electron-Proton Diffraction", DESY **95-228**.
7. H1 Collaboration, S. Aid et al., , Z. Phys **C69** (1995) 27.
8. ZEUS Collaboration, M. Derrick et al., , Z. Phys **C63** (1994) 391.
9. H1 Collaboration, S. Aid et al., Nucl. Phys. **B463** (1996) 3.
10. ZEUS Collaboration, M. Derrick et al., Z.Phys. **C69** (1995) 39.
11. A. Donnachie, P. Landshoff, Phys. Lett. **B296** (1992) 227.
12. H1 Collaboration, I. Abt et al., "The H1 Detector at HERA", DESY **93–103**.
13. G. Ingelman and P. Schlein, Phys. Lett. **B152** (1985) 256.
14. B. List, Diploma Thesis, Techn. Univ. Berlin, unpublished (1993).
15. See for example P. Collins, "An Introduction to Regge Theory & High Energy Physics", Cambridge University Press, Cambridge (1977).
16. N. Nikolaev and B. Zakharov, Z. Phys. **C53** (1992) 331.
17. NMC Collaboration, M. Arneodo et al., Phys. Lett. **B364** (1995) 107;
    BCDMS Collaboration, A. Benevuti et al., Phys. Lett. **B223** (1989) 485.
18. C. Pascaud, F. Zomer, LAL preprint LAL/94-42.
19. Yu. Dokshitzer, JETP **46** (1977) 641.
    V. Gribov and L. Lipatov, Sov. Journ. Nucl. Phys. **15** (1972) 78.
    G. Altarelli and G. Parisi, Nucl. Phys. **B126** (1977) 298.
20. L. Trentadue and G. Veneziano, Phys. Lett. **B323** (1994) 201.
21. H1 Collaboration, T. Ahmed et al., "A Measurement and QCD Analysis of the Proton Structure Function $F_2(x, Q^2)$ at HERA", DESY **96-039**.
22. S. Tapprogge, J. Theissen, A. Valkarova, this report.
23. W. Buchmüller and A. Hebecker, Phys. Lett. **B355** (1995) 573.
24. P. Newman, "A Study of the Dynamics of Diffractive Photoproduction at HERA", PhD Thesis, University of Birmingham (February 1996), RAL-TH-96-011.
25. For a review, see K. Goulianos, Phys. Rep. **101** (1983) 169.
26. D. Roy and R. Roberts, Nucl. Phys. **B77** (1974) 240.
27. T. Chapin et al., Phys. Rev. **D31** (1985) 17.